Synthesis and Characterization of Aqueous Carboxyl-Capped CdS Quantum Dots for Bioapplications

Hui Li

Department of Materials Science and Engineering, Drexel University, Philadelphia, Pennsylvania 19104

Wan Y. Shih

School of Biomedical Engineering, Science, and Health Systems Drexel University, Philadelphia, Pennsylvania 19104

Wei-Heng Shih*

Department of Materials Science and Engineering, Drexel University, Philadelphia, Pennsylvania 19104

A direct and environmentally friendly synthesis method was developed to produce aqueous CdS quantum dots (QDs) at room temperature. The transmission electron microscopy (TEM) and X-ray diffraction (XRD) results showed the small size and the cubic zinc blende structure of the nanocrystals. The quantum yield was comparable to that of the commercial core−shell QDs. With 3-mercaptopropionic acid (MPA) as the capping molecule, the feasibility of using the aqueous CdS QDs as imaging tool was demonstrated with *Salmonella typhimurium* cells. The photoluminescence (PL) properties of the present aqueous CdS QDs can be optimized by adjusting various processing parameters. The emission was due to trap states and was related to the dispersion condition. In particular, with higher pH and MPA/Cd ratio of 2, the QDs exhibited stronger emission. The temperature- and concentration-dependent properties of QDs resulted from the intrinsic interactions between nanoparticles. The aqueous CdS QDs displayed long lifetime of 12 h under UV light and excellent stability in DI water, PBS, and cytosol for more than 26 days. The ease of processing and good PL properties of the aqueous CdS QDs provide a practical and economical approach for single-target imaging application.

1. Introduction

Fluorescent probes are powerful imaging and tracking tools for a wide range of biomedical applications such as disease diagnoses and prognoses, tracking cell/protein interactions, and cell vitality. Traditional organic dyes are limited by their short lifetime, narrow excitation range, and low fluorescence intensity. Quantum dots (QDs) are semiconductor nanocrystals with a typical size of 2−10 nm. In the past decade, the development of QDs as an imaging tool has generated much interest. In comparison with organic dyes, QDs have tunable fluorescence signatures,[1] broad excitation but specific emission spectra, bright emission, and good photostability.[2] Using QDs as the fluorescence marker has the potential for both static[3] and kinetic in-vivo imaging.

The group II−VI nanocrystals such as CdSe, CdTe, CdS,[4,5] ZnS,[6] and ZnSe have been studied extensively, and QDs with a CdSe core and a ZnS shell are currently commercially available. The traditional synthesis method first developed by Murray et al.[7] involves the pyrolysis of dimethyl cadmium ($Cd(CH_3)_2$) within tri-*n*-octylphosphine (TOP) and tri-*n*-octylphosphine oxide (TOPO) to form CdSe nanocrystals. With the diethylzinc and hexamethyldisilathiane precursors, the ZnS capping on CdSe was then achieved[8] to eliminate the broad-band emission and to improve the quantum yield. An epitaxial growth method of the shell has also been established to further improve the photoluminescence properties and stability of the CdSe/ZnS QDs.[9] However, the organic solvent approach was complex and harmful to the environment because of the pyrolysis of toxic organometallic reagents. More recently, the synthesis of CdS,[10] CdSe,[11] and CdTe[12] QDs using CdO as precursor in organic solvent was performed by Peng[13] as a relatively "greener" chemical approach.

For biomedical applications, Gerion et al. made QDs water-soluble by adding a silica shell.[14] The 3-(mercaptopropyl) trimethoxysilane (MPS) replaces the TOPO molecules on the surface, forming a polymerization layer by hydrolysis and silanization. With further functionalization with thiol or amine groups, the surface of QDs is suitable for biomolecule immobilization. However, this process involves multiple steps to bring the QDs into aqueous solvent and to control the growth of shell with many different precursors.

For water-based QDs, Vossmeyer et al.[15] examined the aqueous synthesis of CdS nanoclusters using $Cd(C1O_4)\cdot 6H_2O$, H_2S, and 1-thioglycerol and showed the size dependence of UV−vis absorption. However, no photoluminescence properties were reported. Later, Rogach et al.[16] and Gao et al.[17] described the synthesis of CdTe nanocrystals in an aqueous solution by the reaction between Cd^{2+} and NaHTe. This method required the complex preparation of the Te precursor NaHTe, where H_2Te was first generated by the reaction between Al_2Te_3 and H_2SO_4, followed by titration into NaOH solution under N_2 atmosphere to obtain NaHTe. In addition, the synthesis of CdTe QDs required reflux at 96 °C for hours to obtain the photoluminescence emission. The CdTe QDs capped with 2-mercaptoethanol had the broad-band emission at large wavelengths. There remains a need to develop a direct aqueous synthesis route that is environmentally friendly to produce highly luminescent water-soluble QDs.

In this paper, we described a simple one-step aqueous synthesis method to produce CdS nanocrystals[18] using 3-mer-

* To whom correspondence should be addressed. Tel: (215) 895-6636. Fax: (215) 895-6760. E-mail: shihwh@drexel.edu.

10.1021/ie060963s CCC: $37.00
Published on Web 02/27/2007

captopropionic acid (MPA) as the capping molecule. MPA served both as a stabilizer to disperse QDs and as a linker for conjugation with biomolecules. It was found that the obtained CdS nanocrystals exhibited trap-state emission with strong fluorescence intensity. The emission bandwidth was wide and the photoluminescence intensity was high because of the good dispersion property of MPA. The quantum yield of the CdS QDs was 6.0% as measured using the procedure described by Williams et al.[19] Imaging application of these CdS QDs was demonstrated with *Salmonella typhimurium* cells. Furthermore, we investigated the effects of several processing parameters on the photoluminescence properties of the CdS QDs, including the sonication time, the refrigeration condition, the synthesis atmosphere, the pH, the suspension temperature, the precursor concentration, and the MPA/Cd molar ratio.

2. Materials and Experiments

All chemicals were used as purchased without further purification. The typical synthesis procedure is described as follows. Appropriate amounts of cadmium nitrate [$Cd(NO_3)_2$], sodium sulfide [Na_2S], and 3-mercaptopropionic acid [MPA] (Alfa Aesar, Ward Hill, MA) were first dissolved in deionized (DI) water separately. The $Cd(NO_3)_2$ solution was then dropped into the MPA solution slowly with continuous stirring at room temperature. The ammonium hydroxide [NH_4OH] (Alfa Aesar, Ward Hill, MA) was used to adjust the pH to between 9 and 10. After the quick addition of the Na_2S solution with constant stirring, a clear yellowish suspension of CdS QDs was obtained. For the comparison purpose, another capping molecule, 2-mercaptoethanol (ME) (Pierce Biotechnology, Rockford, IL), was also used. The procedures used for ME were the same as those for MPA. Sonication was carried out when desired using the Ultrasonic Homogenizer 4710 series (Cole-Parmer Instrument Co., Chicago, IL). Suspensions were filtered using syringe filters (Whatman Inc., Florham Park, NJ) or centrifugal filters (Millipore Co., Billerica, MA) of various pore sizes when necessary. Syntheses in N_2 atmosphere were performed in a sealed glove bag (Fisher Scientific, Fairlawn, NJ) flown with nitrogen at room temperature. The aqueous CdS QDs suspension was quenched to 0 °C in a freezer and was stored in a refrigerator at 4 °C.

A JEOL 2000FX electron microscope operating at 200 kV was used for transmission electron microscopy (TEM). Samples were prepared by dropping the CdS QDs suspension on the surface of carbon-coated copper grid and drying it in air. Powder X-ray diffraction patterns were collected on a Siemens D 500 X-ray diffractometer operated in the Bragg configuration using Cu Kα radiation. The accelerating voltage was set at 40 kV with a 30 milliamp flux. The scanning step was 0.05° and the duration of the step was 1 s. The X-ray powder sample was precipitated from the QDs suspension by the addition of ethanol followed by centrifugation and air-drying at 50 °C overnight.

Photoluminescence spectra of the QDs suspensions were obtained using a QM-4/2005 spectrofluorometer (Photon Technology International, Birmingham, NJ) with a 10-mm plastic cuvette. Background corrections were carried out to remove the wavelength dependence of the detector. For a given suspension, the emission spectra were collected with the optimal excitation wavelength. Optical absorption experiments were carried out on a Lambda-40 UV−Vis spectrometer (PerkinElmer Life And Analytical Sciences Inc., Waltham, MA). The size distribution of QDs in aqueous suspension was measured by dynamic light scattering with a Zetasizer Nano ZS (Malvern Instruments Ltd., Worcestershire, United Kingdom).

To obtain the quantum yield of the present aqueous CdS QDs, Rhodamine 101 (Fisher Scientific, Fairlawn, NJ) was used as a standard. The commercial EviTags core−shell CdSe/ZnS QDs (Evident Technologies Inc., Troy, NY) were also included for comparison. The absorbance and the emission spectra of each system were measured with a fixed excitation wavelength of 365 nm at several dilute concentrations. The wavelength of 365 nm was chosen because it was the proper excitation wavelength for all the samples. To minimize potential reabsorption,[20] the absorbance was kept below 0.15 to avoid any effect because of concentration. The integrated fluorescence intensity was obtained by integrating the emission intensity over the entire area under the emission peak.

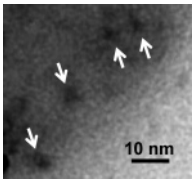

Figure 1. TEM image of CdS QDs exhibited individual particles of a few nanometers.

To conjugate the QDs with *Salmonella t.* cells (KPL, Gaithersburg, MD), the carboxyl group of the capping MPA on the QD surface was first activated using 1-ethyl-3(3-dimethylaminopropyl) carbodiimide (EDC) and *N*-hydrocyl-sulfo-succinimide (sulfo-NHS). The unreacted chemicals and excess byproducts were removed by the 100 kD Nanosep and Nanosep MF centrifugal device (Pall Co., East Hills, NY) at 10000 rpm with a microcentrifuge. The activated QDs were then mixed with *Salmonella t.* antibody, CSA-1 (KPL, Gaithersburg, MD), in PBS with roughly the QD to antibody number ratio of 2. After reaction and conjugation through peptide bonding, the unbound antibodies and unbound QDs were removed by microcentrifugation at 10000 rpm with the 300 kD Nanosep and Nanosep MF centrifugal device (Pall Co., East Hills, NY). Then, the antibody-conjugated QDs were mixed with *Salmonella t.* cells suspension, and they attached to the cells through the specific antibody. At the end, the *Salmonella t.* cells with tagged QDs were collected by microcentrifugation, and the supernatant was discarded. The collected cells were rinsed with DI water and were centrifuged three times to remove the salt and the excess unbound antibody-QDs. The *Salmonella t.* cells tagged with QDs were visualized with a Leica DMRX upright microscope (Leica Microsystems GmbH, Wetzlar, Germany) equipped with the appropriate fluorescence filters. Digital images were acquired using a Leica DC 300FX camera (Leica Camera AG, Solms, Germany).

3. Results and Discussions

3.1. Size and Structure of Nanocrystals. Transmission electron microscopy was used to image the as-synthesized CdS QDs. Figure 1 is a TEM image showing individual particles which have the size of 2−5 nm. This is consistent with the filtering results which showed that most of the QDs can pass through 50 kD filter with the pore size of 5 nm. We have also imaged the nanoparticles on silicon substrate using an atomic force microscope (AFM), which also indicated that the QDs were 2−6 nm in size (not shown). The X-ray powder diffraction pattern of CdS QDs is shown in Figure 2, which shows that the CdS has a cubic zinc blend crystalline structure, and the crystalline size is estimated to be about 2 nm according to the Scherrer's formula.[21]

3.2. Quantum Yield. In Figure 3, we plot the integrated emission intensity versus absorbance for Rhodamine 101,

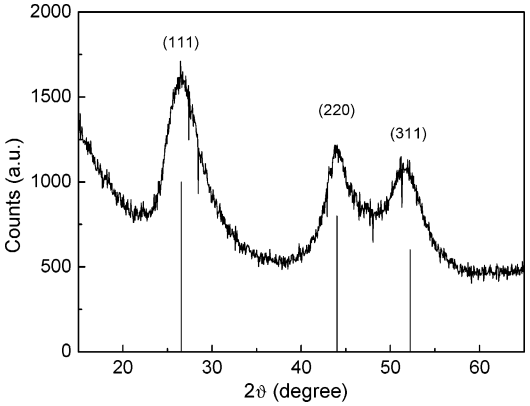

Figure 2. XRD spectrum of CdS QDs with the lines indicating the pattern and relative intensities of bulk CdS with cubic zinc blende structure.

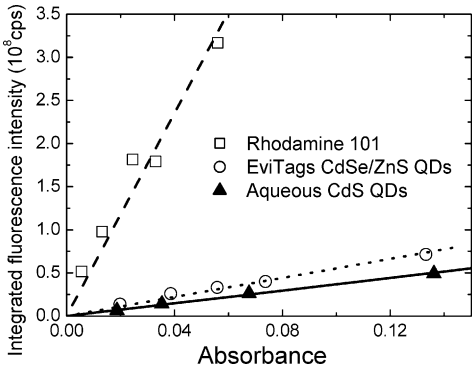

Figure 3. Integrated photoluminescence intensity versus absorbance for Rhodamine 101, EviTags CdSe/ZnS QDs, and the present aqueous CdS QDs. The slope gives the quantum yield as depicted by eq 1.

EviTags CdSe/ZnS QDs, and the present aqueous CdS QDs. The quantum yield, ϕ_X, can be expressed as[19]

$$\phi_X = \phi_{ST}\left(\frac{\mathrm{Grad}_X}{\mathrm{Grad}_{ST}}\right)\left(\frac{\eta_X^2}{\eta_{ST}^2}\right) \quad (1)$$

where ϕ_X (ϕ_{ST}), Grad_X (Grad_{ST}), and η_X (η_{ST}) denote, respectively, the quantum yield, the slope of the integrated emission intensity versus absorbance, and the solvent refractive index of the test sample (the standard). In the experiment, Rhodamine 101 was dissolved in ethanol ($\eta_{ethanol} = 1.36$) as the standard sample with the known quantum yield of 100%.[22] The EviTags CdSe/ZnS QDs and the aqueous CdS QDs were dispersed in DI water ($\eta_{water} = 1.33$). Using eq 1, we obtained the quantum yield of 8.9% and 6.0% for the EviTags CdSe/ZnS QDs and the CdS QDs, respectively. It is encouraging that with the present aqueous synthesis route, we have produced CdS QDs without shells displaying the quantum yield comparable to that of the commercial core−shell QDs. It is possible to further improve the quantum yield by adding a shell to the present aqueous QDs, since it is well-known that the core−shell structure enhances the quantum yield of QDs.[8,9]

3.3. Imaging of *Salmonella t.* Cells. The present MPA-capped CdS QDs exhibited strong visible photoluminescence that can be used as an imaging tool for single targets. Moreover, the carboxyl group of MPA can be readily conjugated with any amine-containing biomolecules through peptide bonding, an advantage over the organic QDs that have no functionalized surfaces for direct conjugation. As an example, we carried out the imaging test for *Salmonella t.* cells using the MPA-capped CdS QDs as described in section 2. A drop of the QD-bound *Salmonella t.* suspension was placed on a glass slide covered with a cover glass and was placed in the fluorescence microscope. The image of the *Salmonella t.* cells under the normal light and that under the fluorescence mode are shown in Figure 4a and Figure 4b, respectively. As can be seen, under the fluorescence mode, the otherwise invisible cells were lighted up by the QDs, and the fluorescence image of the cells matched that of the cells under the normal light, indicating that the present aqueous QDs could indeed be used to image biological systems. The blue tint of the image came from the fluorescence filter that we used.

3.4. Effect of Capping Molecules. In the synthesis of aqueous CdS QDs, MPA was used as the capping molecule to disperse the nanoparticles in the suspension and to control the particle size. The thiol group of the MPA attached to the Cd cations on the particle surface and the carboxyl group on the other end of the MPA were fully charged at high pH as illustrated in the schematics of Figure 5a and Figure 5b. Conceivably, that MPA was fully charged at high pH was an important factor of the colloidal stability of the QDs as well as QDs' particle size. To investigate the effect of capping molecules on QDs' size and colloidal stability, we have also synthesized QDs with ME as the capping molecules. In Figure 6a, the absorption spectrum and the PL intensity spectrum of the ME-capped CdS QDs are shown together with those of the MPA-capped QDs. As can be seen, the ME-capped QDs exhibited a much lower PL intensity than the MPA-capped QDs. In addition, the absorption edge of the ME-capped QDs was smaller than that of the MPA-capped QDs, indicating that the ME-capped CdS QDs were smaller than the MPA capped QDs. According to the relationship between the band edge energy shift and the particle size,[1] we estimated the primary particle size of the ME-capped QDs to be 2.9 nm, smaller than that of the MPA-capped QDs, 3.2 nm. Dynamic light scattering experiments were carried out to measure particle size in the suspension, and the result is shown in Figure 6b. As can be seen, the MPA-capped QDs had the mean size of 6.3 nm, while the ME-capped QDs had the mean size of 31.0 nm. Apparently, the mean sizes of both samples were larger than their primary particle sizes as deduced from the absorption edge, indicating that both ME-capped and MPA-capped QDs aggregated to some degree in the suspensions. Moreover, the cluster size of the ME-capped QDs was larger than that of the MPA-capped QDs, indicating that the ME-capped QDs were more prone to aggregation than MPA-capped QDs. This difference may be attributed to the fact that MPA was more highly charged than ME at the same pH to better maintain the colloidal stability of the QDs. The lower PL of the ME-capped QDs may be contributed to their higher degree of clustering. The proximity to other QDs in a cluster provided more dissipation paths, which could suppress the emission. Furthermore, because of the proximity, the emission of one QD could also be absorbed by another QD and be dissipated nonradioactively to result in a reduced PL intensity.[23]

The emission peak of the present aqueous CdS QDs was about 1 eV lower than the absorption edge, indicating that the emissions of the present QDs were not band-edge emissions and that trap states were involved in the emission. It is likely that the trap states involved were not surface trap states as one should immediately suspect as most of the trap states involved in the QDs synthesized by the organic route were surface trap states. If the present trap-state emission were indeed surface-trap-state emission, the emission intensity would have increased with a decreased primary QD particle size (increased

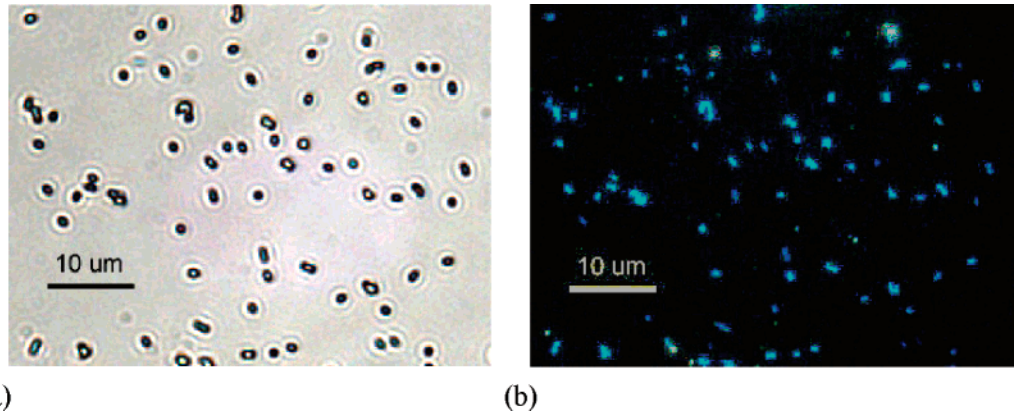

Figure 4. Imaging of *Salmonella t.* cells by the aqueous CdS QDs: (a) optical micrograph under normal white light and (b) optical micrograph obtained in fluorescent mode.

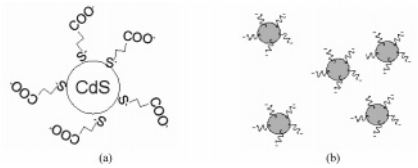

Figure 5. (a) A schematic of MPA bound to a CdS particle through the thiol group and (b) a schematic of CdS particles stabilized by the negatively charged MPA on the surface at high pH.

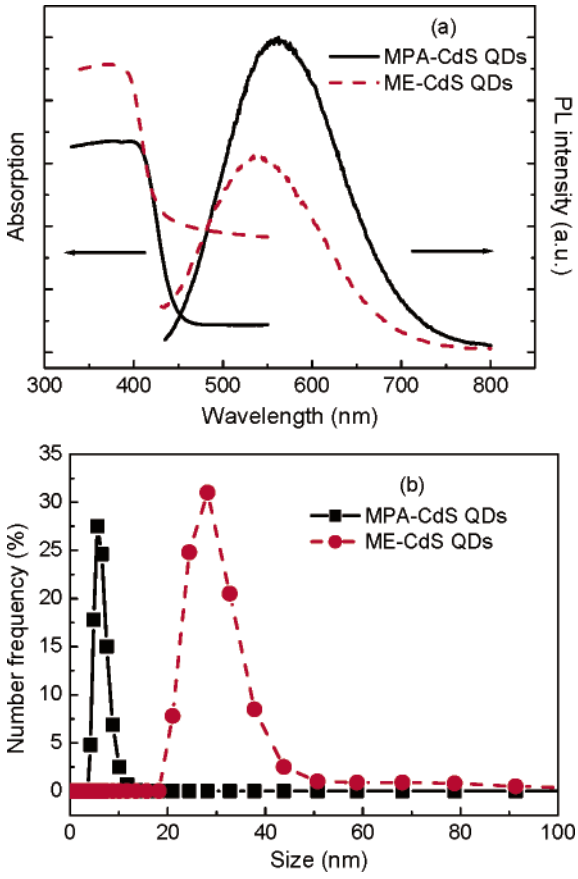

Figure 6. (a) Absorption and PL emission spectra of CdS QDs synthesized with different capping molecules and (b) size distribution of CdS QDs with different capping molecules measured by dynamic light scattering.

surface area). To the contrary, the present aqueous QDs showed the opposite trend: the MPA-capped QDs, though larger, exhibited higher emission intensity than the ME-capped QDs. Furthermore, in an earlier publication, the emission of CdS colloidal particles synthesized in water was found 0.9 eV lower

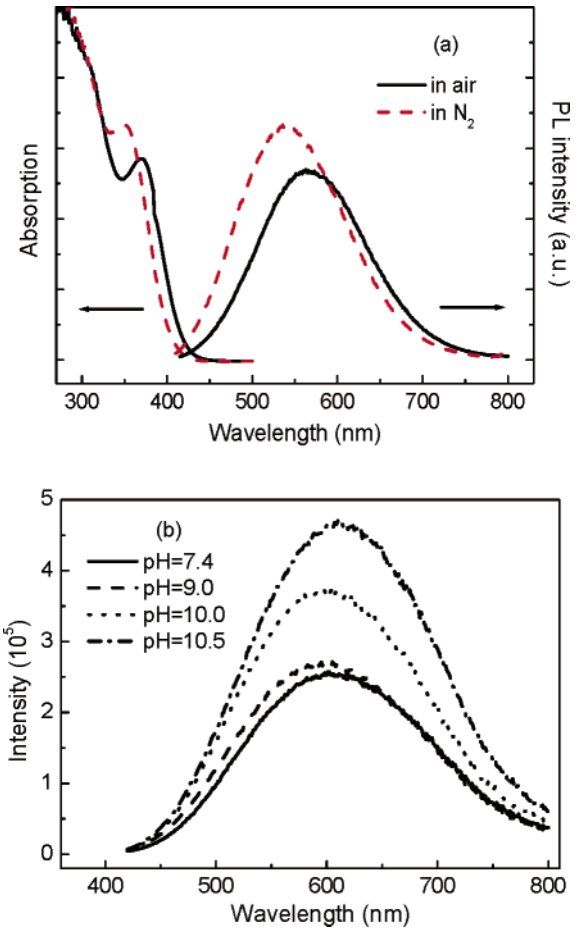

Figure 7. Effects of (a) atmosphere and (b) pH on the PL properties of the CdS QDs.

than the band-edge emission and was attributed to bulk-trap-state emissions involving the recombination of electrons with holes at sulfur vacancies.[24] Given the Cd-rich synthesis environment of the present aqueous QDs, it is likely that sulfur vacancies existed in the present QDs and that the observed trap-state emission could be sulfur vacancy related bulk trap-state emissions similar to those found in colloidal CdS.[24] In addition, as can be seen from Figure 6a, both the absorption edge and emission wavelength of the ME-capped CdS QDs were smaller than those of the MPA-capped QDs. This indicated that the trap-state emission of the present QDs was size-dependent. This was consistent with a recent study which showed that along with

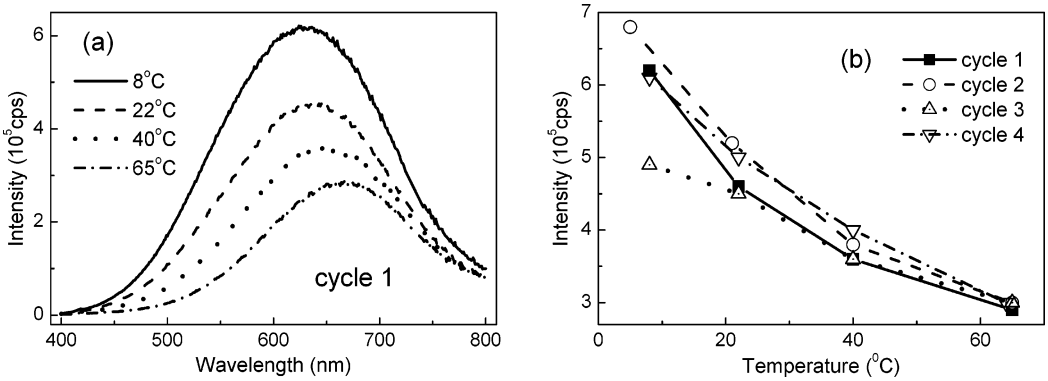

Figure 8. Temperature effect to the PL properties of CdS QDs: (a) emission spectra at different temperature in the first cycle and (b) emission peak intensity versus temperature for four cycles.

band edges, the energies of trap states could also change with particle size to result in particle-size-dependent trap-state emissions.[25]

3.5. Effect of Processing Parameters. We examined the effects of several processing variables, including the sonication time, the refrigeration conditions, the synthesis atmosphere, and the pH on the PL properties of the aqueous CdS QDs. Compared with samples prepared without sonication, the sample sonicated for 5 min exhibited about 20-nm red-shift in the emission spectrum. This can be explained by the increased suspension temperature which promoted further particle growth during the sonication process. Although conventional sonication may break up agglomerates and result in smaller particles, it applies to systems where particle nucleation and growth occur at high temperature. However, the present aqueous CdS QDs nucleated and grew at room temperature. A slight increase in temperature could have a significant impact on the particle size to affect the emission peak wavelength. In contrast to sonication, refrigeration had the opposite effect on the PL properties of QDs. The sample refrigerated at 4 °C for 28 days exhibited an emission peak wavelength 20 nm smaller than that of the sample stored at room temperature. The lower temperature in a refrigerator apparently slowed the growth of QDs.

The synthesis atmosphere played an important role in the formation and stability of the QDs. As shown in Figure 7a, the QDs synthesized in N_2 had both the absorption edge and emission peak blue-shifted relative to those of the QDs synthesized in air. According to Aldana et al.'s study,[26] in the presence of both light and oxygen, the thiol groups of two adjacent MPA molecules can react to form a disulfide bond and can dissociate from the QD surface. Therefore, the QDs synthesized in air would grow to a larger size, exhibiting a red-shifted absorption edge. The emission wavelength of QDs in air was larger than that of the QDs in N_2 as well, consistent with the particle growth behavior.

Figure 7b shows that increasing the solution pH during synthesis increased the emission intensity of the CdS QDs. This can be understood by the properties of MPA. The pKa of the thiol group is about 8.3.[27] At higher pH, more thiol groups became dehydrogenated, which was expected to strengthen the covalent bonding between MPA and Cd^{2+} on the surface of QDs. In addition, the higher pH promoted the negative charge of carboxyl groups of MPA and helped disperse the nanoparticles better. Furthermore, the solubility of CdS decreased with increasing pH,[28] which benefited the nucleation and growth of QDs and therefore generated more nanoparticles. All these effects would help improve the PL intensity of QDs at higher pH.

3.6. Effect of Temperature. After synthesis, we examined the temperature dependence of the photoluminescence behavior

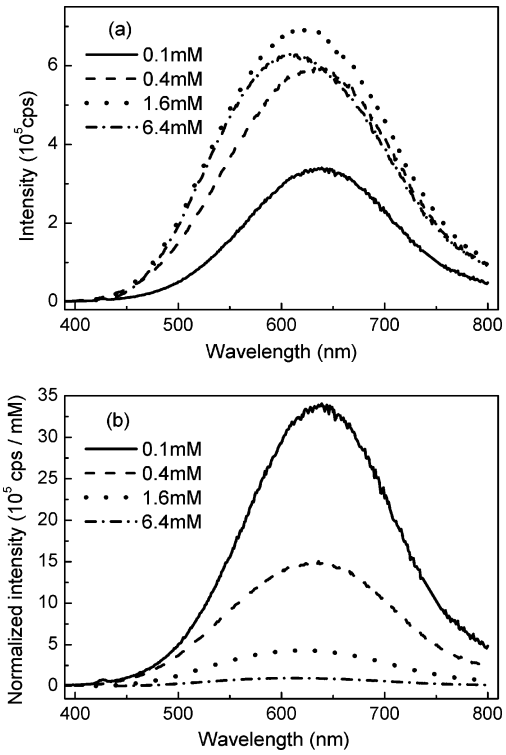

Figure 9. Concentration effect to the PL properties of CdS QDs: (a) emission spectra and (b) normalized emission spectra at various concentrations, where the normalized emission spectra represent the ratio of emission intensity over concentration versus wavelength.

of the CdS QDs. In Figure 8a, we plot the PL emission spectra of the CdS QDs obtained at 8, 22, 40, and 65 °C. It is shown that with increasing temperature, the emission intensity decreased, the emission peak shifted to larger wavelength, and the full width at half maximum (FWHM) reduced. The above behavior was reversible and repeatable for four successive cycles of temperature change. Between any consecutive cycles, the sample was stored at 4 °C overnight. As shown in Figure 8b, for all cycles, the emission intensity followed the same temperature-dependent trend. Similar emission intensity decrease with increasing temperature was recently reported in the range of 25−80 °C for CdSe QDs.[29] The phenomenon was attributed to the localization of electrons in the interfacial trap states at higher temperature. Therefore, the electron−hole pairs transferred energy in a nonradioactive mode rather than contributing to PL emission by the electron−hole recombination. The emission peak shifted to larger wavelength with increasing temperature because of further particle growth of QDs, similar to the effect of sonication. The FWHM, on the other hand, was

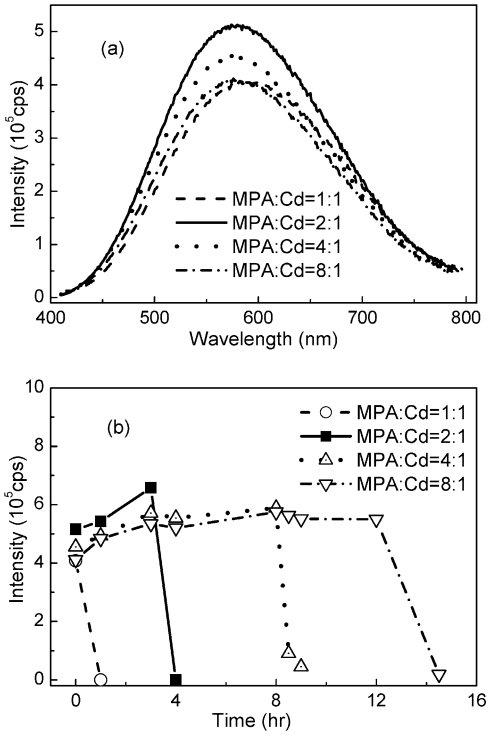

Figure 10. Effect of MPA/Cd molar ratio: (a) emission spectra at 0 h and (b) emission peak intensity versus time.

reduced with increasing temperature. This has been suggested to result from the size and emission suppression of non-predominant sized QDs at higher temperature.[30] More studies need to be performed to elucidate the mechanisms involved in the effect of temperature.

3.7. Effect of Concentration. The PL properties of the QDs were examined for samples with four different CdS precursor concentrations, 0.1 mM, 0.4 mM, 1.6 mM, and 6.4 mM. The emission spectra measured at 8 °C are shown in Figure 9a, where we can see that the emission intensity did not increase in proportion to the concentration. The 1.6 mM sample exhibited the highest emission intensity, even higher than the 6.4 mM sample. This is contrary to one's intuition that the sample with the highest concentration should exhibit the highest emission intensity. To better illustrate the concentration effect, we plot the concentration-normalized emission spectra in Figure 9b, which shows that the normalized emission intensity decreased with increasing QD concentration. The concentration dependence of PL intensity was reversible.

There are several reasons contributing to this interesting phenomenon. We found that after the excess MPA and other ions in the suspension were removed by dialysis, the PL intensity increased by more than 30% even though the QD concentration remained the same. It suggested that, for the as-synthesized QDs with higher concentration, the emission intensity was reduced in part because of higher concentration of excess MPA and other ions in the suspension. On the other hand, higher concentration might promote the formation of QDs clusters. The poor dispersion would reduce the PL intensity as well, which was consistent with the discussion in the comparison of MPA-capped and ME-capped QDs.

3.8. Effect of MPA/Cd Molar Ratio. As capping molecule, MPA stabilized the nanocrystals in the aqueous suspension. With the same CdS QD concentration (1.6 mM), several batches of samples were synthesized with different MPA/Cd molar ratios, and their effect on the emission of QDs is shown in Figure 10a. As can be seen, the ratio of MPA/Cd = 2 was optimal to obtain the highest emission intensity. At MPA/Cd = 1, the intensity was lower than that at MPA/Cd = 2, because the CdS QDs were not covered by MPA sufficiently. Possibly, more clusters of QDs were generated because of poor dispersion, and the emission intensity was reduced by nonradioactive energy transfer. On the other hand, at MPA/Cd = 4 and 8, too many MPA molecules in the suspension resulted in lower emission intensity as well, which is consistent with the observation in the concentration effect.

However, the excess MPA could help improve the photostability of QDs significantly. As shown in Figure 10b, under continuous UV illumination the sample with higher MPA/Cd ratio exhibited longer lifetime. With MPA/Cd = 8, the CdS QDs were stable for more than 12 h, while the sample with MPA/Cd = 1 could only withstand for less than 1 h. The PL intensity eventually vanished, because the coexistence of UV light and oxygen led to the gradual photooxidation of MPA and the generation of disulfides, resulting in agglomeration, settling, and eventual degradation of QDs. However, in the absence of light, the aqueous CdS QDs suspension remained stable for more than 12 months at 4 °C.

3.9. Colloidal Stability and Photostability in PBS and Cytosol. The QDs have the advantage of long lifetime under UV over organic dyes, and therefore they can be used as fluorescent label to examine the long-term kinetics of molecular/cellular interactions. The colloidal and optical stability of QDs in a biological system is also critical. To examine the stability of the present CdS QDs, we mixed 1.6 mM suspension at the volume ratio of 1:3 with DI water, phosphorus buffer solution (PBS, 1×), and cytosol (cell line U937, 10^6 cells/mL). The cytosol was prepared by heating and cooling the cells repeatedly, breaking the cell membrane, and extracting the cytoplasm from supernatant after centrifugation. The three mixture samples were stored at 4 °C in darkness and their PL properties were monitored for up to 26 days. Figure 11a shows the initial emission spectra of the three mixtures, and Figure 11b shows the change of emission peak intensity over time. Clearly, all three samples remained stable for more than 26 days. Therefore, the present aqueous CdS QDs were demonstrated to have

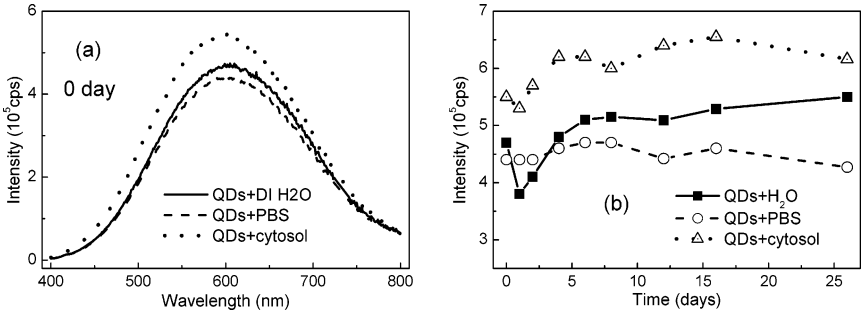

Figure 11. Stability of aqueous CdS QDs in DI water, PBS, and cytosol: (a) emission spectra on day 0 and (b) emission peak intensity versus time.

excellent stability in DI water, saline solution, and cytosol, showing their potential applications in long-term biological imaging and tracking experiments.

4. Conclusions

A direct and environmentally friendly synthesis method was developed to produce aqueous CdS QDs at room temperature. The TEM and X-ray diffraction (XRD) results showed the small size and cubic structure of the nanocrystals. The quantum yield was comparable to that of the commercial core−shell QDs. Despite that the emission was trap-state emission in nature, the MPA-capped QDs were bright and could be used for bioimaging applications. The PL properties of the present aqueous CdS QDs can be optimized by adjusting the capping molecules and various processing parameters. It was shown that the emission wavelength was size-dependent and that better dispersion condition led to stronger PL. Particularly, with higher pH and MPA/Cd ratio of 2, the QDs exhibited higher emission intensity. The temperature- and concentration-dependent properties of QDs resulted from the intrinsic interactions between nanoparticles. The PL was sensitive to temperature, and the change with temperature was reversible and repeatable after heating cycles, which can be used for certain detection. The aqueous CdS QDs displayed long lifetime of 12 h under UV light and excellent stability in DI water, PBS, and cytosol for more than 26 days. The ease of processing and good PL properties of the aqueous CdS QDs provide a practical and economical approach for single-target-imaging application.

Acknowledgment

This work is supported in part by the National Institute of Health (NIH) under Grant No. 1 R01 EB000720, the Environmental Protection Agency (EPA) under Grant No. R8296040, and the Nanotechnology Institute. We thank Melissa Schillo and David Zimmerman for their help in the preliminary part of the work. We thank Dr. Noreen Robertson for preparing the cytosol used in the stability study. We thank Dr. Steve Wrenn for his help on the UV−Vis absorption measurement and Dr. Margaret Wheatley for her help on the dynamic light scattering experiment. We also thank Dr. Mengyan Li for her help in taking the fluorescence pictures and Dr. Hongyu Luo for helping in taking the TEM image.

Literature Cited

(1) Brus, L. E. Electron-Electron and Electron-Hole Interactions in Small Semiconductor Crystallites: the Size Dependence of the Lowest Excited Electronic State. *J. Chem. Phys.* **1984**, *80* (9), 4403−4409.

(2) Chan, W. C. W.; Maxwell, D. J.; Gao, X.; Bailey, R. E.; Han, M.; Nie, S. Luminescent Quantum Dots for Multiplexed Biological Detection and Imaging. *Curr. Opin. Biotechnol.* **2002**, *13*, 40−46.

(3) Seydel, C. Quantum Dots Get Wet. *Science* **2003**, *300* (5616), 80−81.

(4) Foglia, S.; Suber, L.; Righini, M. Size Tailoring of CdS Nanoparticles by Different Colloidal Chemical Techniques. *Colloid Surf.* **2001**, *177*, 3−12.

(5) Li, Z.; Du, Y. Biomimic Synthesis of CdS Nanoparticles with Enhanced Luminescence. *Mater. Lett.* **2003**, *57*, 2480−2484.

(6) Kho, R.; Torres-Martinez, C. L.; Mehra, R. K. A Simple Colloidal Synthesis for Gram-Quantity Production of Water-Soluble ZnS Nanocrystal Powders. *J. Colloid Interface Sci.* **2000**, *227*, 561−566.

(7) Murray, C. B.; Norris, D. J.; Bawendi, M. G. Synthesis and Characterization of Nearly Monodisperse CdE (E=S, Se, Te) Semiconductor Crystallites. *J. Am. Chem. Soc.* **1993**, *115*, 8706−8715.

(8) Dabbousi, B. O.; Rodriguez-Viejo, J.; Mikulec, F. V.; Heine, J. R.; Mattoussi, H.; Ober, R.; Jensen, K. F.; Bawendi, M. G. (CdSe)ZnS Core-Shell Quantum Dots: Synthesis and Characterization of a Size Series of Highly Luminescent Nanocrystallites. *J. Phys. Chem. B* **1997**, *101*, 9463−9475.

(9) Peng, X.; Schlamp, M. C.; Kadavanich, A. V.; Alivisatos, A. P. Epitaxial Growth of Highly Luminescent CdSe/CdS Core/Shell Nanocrystals with Photostability and Electronic Accessibility. *J. Am. Chem. Soc.* **1997**, *119*, 7019−7029.

(10) Yu, W.; Peng, X. Formation of High-Quality CdS and Other II-VI Semiconductor Nanocrystals in Noncoordinating Solvents: Tunable Reactivity of Monomers. *Angew. Chem., Int. Ed.* **2002**, *41*, 2368−2371.

(11) Qu, L.; Peng, X. Control of Photoluminescence Properties of CdSe Nanocrystals in Growth. *J. Am. Chem. Soc.* **2002**, *124*, 2049−2055.

(12) Peng, Z.; Peng, X. Formation of High-Quality CdTe, CdSe, and CdS Nanocrystals Using CdO as Precursor. *J. Am. Chem. Soc.* **2001**, *123*, 183−184.

(13) Peng, X. Green Chemical Approaches Toward High-Quality Semiconductor Nanocrystals. *Chem. Eur. J.* **2002**, *8*, 335−339.

(14) Gerion, D.; Pinaud, F.; Williams, S. C.; Parak, W. J.; Zanchet, D.; Weiss, S.; Alivisatos, A. P. Synthesis and Properties of Biocompatible Water-Soluble Silica-Coated CdSe/ZnS Semiconductor Quantum Dots. *J. Phys. Chem. B* **2001**, *105*, 8861−8871.

(15) Vossmeyer, T.; Katsikas, L.; Gienig, M.; Popovic, I. G.; Diesner, K.; Chemseddine, A.; Eychmiiller, A.; Weller, H. CdS Nanoclusters-Synthesis, Characterization, Size-Dependent Oscillator Strength, Temperature Shift of the Excitonic-Transition Energy, and Reversible Absorbency Shift. *J. Phys. Chem.* **1994**, *98*, 7665−7631.

(16) Rogach, A. L.; Katsikas, L.; Kornowski, A.; Su, D.; Eychmuller, A.; Weller, H. Synthesis and Characterization of Thiol-Stabilized CdTe Nanocrystals. *Ber. Bunsen-Ges. Phys. Chem.* **1996**, *100*, 1772−1778.

(17) Gao, M.; Kirstein, S.; Mohwald, H.; Rogach, A. L.; Kornowski, A.; Eychmuller, A.; Weller, H. Strongly Photoluminescent CdTe Nanocrystals by Proper Surface Modification. *J. Phys. Chem. B* **1998**, *102*, 8360−8363.

(18) Shih, W.-H.; Li, H.; Schillo, M.; Shih, W. Y. Synthesis of Water Soluble Nanocrystalline Quantum Dots and Uses Thereof. U.S. Patent application No. 60/573,804, May 24, 2005.

(19) Williams, A. T. R.; Winfield S. A.; Miller, J. N. Relative Fluorescence Quantum Yields Using a Computer Controlled Luminescence Spectrometer. *Analyst* **1983**, *108 (1290)*, 1067−1071.

(20) Dhami, S.; Mello, A. J. de; Rumbles, G.; Bishop, S. M.; Phillips, D.; Beeby, A. Phthalocyanine Fluorescence at High-Concentration-Dimers or Reabsorption Effect. *Photochem. Photobiol.* **1995**, *61*, 341−346.

(21) Warren, B. E. *X-Ray Diffraction*; Dover: New York, 1990.

(22) Karstens, T.; Kobs, K. Rhodamine B and Rhodamine 101 as Reference Substances for Fluorescence Quantum Yield Measurements. *J. Phys. Chem.* **1980**, *84*, 1871−1872.

(23) Murray, C. B.; Kagan, C. R.; Bawendi, M. G. Synthesis and Characterization of Monodisperse Nanocrystals and Close-Packed Nanocrystal Assemblies. *Annu. Rev. Mater. Sci.* **2000**, *30*, 545−610.

(24) Zhao, X.; Schroeder, J.; Persans, P. D.; Bilobeau, T. G. Resonant-Raman-Scattering and Photoluminescence Studies in Glass-Composite and Colloidal CdS. *Phys. Rev. B* **1991**, *43*, 12580−12589.

(25) Li, J.; Wei, S.; Wang, L. Stability of the DX^- Center in GaAs Quantum Dots. *Phys. Rev. Lett.* **2005**, *94*, 185501−185504.

(26) Aldana, J.; Wang, Y.; Peng, X. Photochemical Instability of CdSe Nanocrystals Coated by Hydrophilic Thiols. *J. Am. Chem. Soc.* **2001**, *123*, 8844−8850.

(27) http://sakura.cpe.fr/pka.html pKa at 25 °C (accessed May 19, 2006).

(28) http://www.hoffland.net/src/tks/3.xml Sulfide Solubility (accessed May 19, 2006).

(29) Biju, V.; Makita, Y.; Sonoda, A.; Yokoyama, H.; Baba, Y.; Ishikawa, M. Temperature-Sensitive Photoluminescence of CdSe Quantum Dot Clusters. *J. Phys. Chem. B* **2005**, *109*, 13899−13905.

(30) Lubyshev, D. I.; Gonzalez-Borrero, P. P.; Marega, E.; Petitprez, E.; Scala, N. L.; Basmaji, P. Exciton Localization and Temperature Stability in Self-Organized InAs Quantum Dots. *Appl. Phys. Lett.* **1996**, *68* (2), 205−207.

Received for review July 24, 2006
Revised manuscript received January 9, 2007
Accepted January 22, 2007

IE060963S